Available online at www.sciencedirect.com
SCIENCE DIRECT®
Journal of Molecular Spectroscopy 228 (2004) 544–553
Journal of MOLECULAR SPECTROSCOPY
www.elsevier.com/locate/jms

Fourier transform emission spectroscopy and ab initio calculations on NbCl☆

R.S. Ram,[a,*] N. Rinskopf,[b,c] J. Liévin,[b] and P.F. Bernath[a,d]

[a] *Department of Chemistry, University of Arizona, Tucson, AZ 85721, USA*
[b] *Université Libre de Bruxelles, Service de Chimie Quantique et Photophysique, CP 160/09 Av. F. D. Roosevelt 50, Bruxelles, Belgium*
[c] *F.R.I.A. Researcher, Belgium*
[d] *Department of Chemistry, University of Waterloo, Waterloo, Ont., Canada N2L 3G1*

Received 24 September 2003
Available online 6 March 2004

Dedicated to Dr. Jon T. Hougen

Abstract

The emission spectrum of NbCl has been recorded in the 3000–20 000 cm^{-1} region using a Fourier transform spectrometer. The bands were observed by microwave excitation of a mixture of $NbCl_5$ vapor and He. Two groups of bands observed in the 6500–7000 cm^{-1} and 9800–11 000 cm^{-1} regions have been assigned to two electronic transitions. Five bands observed in the 6500–7000 cm^{-1} region consist of R, P, and Q branches with no combination defect or Λ-doubling. They have been assigned as five sub-bands of a $\Delta\Lambda = \pm 1$ transition with $\Lambda > 1$. Nine bands observed in the 9800–11 000 cm^{-1} regions consist of R and P branches, and they are also free from Λ-doubling. These bands have been classified into four sub-bands of a $\Delta\Lambda = 0$ transition (with $\Lambda > 1$), which has tentatively been assigned as $^5\Delta$–$^5\Delta$. The two transitions have no electronic states in common. Ab initio calculations have been performed on NbCl and the spectroscopic properties of the low-lying electronic states have been calculated. The ground state of NbCl has been predicted to be a $^5\Pi$ state arising from the $3\sigma^1\ 1\delta^2\ 2\pi^1$ configuration, with a low-lying $^5\Delta$ state at 1300 cm^{-1} from the $3\sigma^1\ 1\delta^1\ 2\pi^2$ configuration. The results of our experimental and theoretical studies will be presented. This work represents the first experimental investigation of the spectra of NbCl and the first ab initio prediction of the spectroscopic properties of the low-lying electronic states.

Keywords: Fourier transform spectroscopy; Emission spectroscopy; Ab initio calculations

1. Introduction

In recent years a number of transition metal halides have been investigated in the gas phase and their electronic spectra have been characterized at high resolution. These molecules have attracted considerable recent attention because of their chemical and theoretical importance [1]. Spectroscopic studies of these molecules provides insight into chemical bonding in simple metal-containing systems [2]. Because of the high cosmic abundance of transition metal elements in stars, transition metal-containing halides may also be of astrophysical importance.

For the VB group of transition metal halide family, high resolution spectroscopic data are available only for VCl [3,4] and VF [5]. An electronic transition of VCl has recently been observed in the near infrared region and the ground state has been identified as a $^5\Delta$ state based on experimental observations and ab initio calculations [4]. Among the Nb-containing diatomic molecules, spectroscopic data are available for NbO [6] and NbN [7], obtained by optical emission spectroscopy, but the electronic spectra of Nb-containing diatomic halides remain unexplored. A comparative ab initio study of the bond strengths of NbCl and NbF along with other second row transition metal hydrides, fluorides and chlorides has been carried out by Siegbahn [8]. The

☆ Supplementary data associated with this article can be found in the online version, at doi:10.1016/j.jms.2004.02.001.

* Corresponding author. Fax: 1-520-621-8407.
E-mail address: rram@u.arizona.edu (R.S. Ram).

0022-2852/$ - see front matter © 2004 Elsevier Inc. All rights reserved.
doi:10.1016/j.jms.2004.02.001

thermochemical properties of NbF and TaF have been investigated by Galkin et al. [9].

In the present paper we report the first observation of the electronic spectra of NbCl using the technique of Fourier transform emission spectroscopy. In this work we have recorded the high resolution spectra of NbCl and have obtained a rotational analysis of bands belonging to two electronic transitions. We have also carried out ab inito calculations to predict the spectroscopic properties of the low-lying electronic states. The results of our experimental assignments will be discussed in the light of our ab initio results.

2. Ab initio calculations

Large scale ab initio calculations have been performed in order to survey the valence electronic structure of NbCl below 15 000 cm^{-1}. We have used the same computational approach as in our previous work on transition metal diatomic nitrides [10–13], oxides [14], and chlorides [4,15,16]. The ab initio calculation consists of a complete active space self-consistent field (CASSCF) calculation [17] followed by an internally contracted multireference configuration interaction (CMRCI) calculation [18], as implemented in the MOLPRO computer package [19]. The core electrons of both atoms (28 and 10 electrons for Nb and Cl, respectively) are described by quasi-relativistic Wood-Boring pseudopotentials [20,21]. The remaining external electrons (13 and 7 for Nb and Cl, respectively) are described by valence basis sets optimized for the aforementioned core potentials [20,21]. Polarization orbitals are added on both atoms: a single f-type gaussian function (exponent of 0.8) on Nb and two d-type gaussians (exponents of 1.046 and 0.344) on Cl [22].

The CASSCF wavefunctions have been constructed as linear combinations of configuration state functions (CSFs) of a given C_{2v} symmetry, with 20 electrons distributed in the six σ, three π, and one δ molecular orbitals (MOs), correlating with the 4s, 4p, 4d, and 5s orbitals of niobium and the 3s and 3p orbitals of chlorine. Eight electrons were placed in low-lying closed shell MOs, two σ and one π, while the twelve other electrons (active electrons) were distributed in all possible ways among the remaining valence MOs. The size of such CASSCF expansions ranges between 2000 and 5200 CSFs (C_{2v} symmetry) depending on the space and spin symmetries. A state averaging procedure has been used to reproduce the spatial degeneracy for $\Lambda > 0$ and to describe excited states of the same symmetry.

The second step of the computational procedure is a large scale CMRCI calculation using the optimized CASSCF orbitals as the one-electron basis set. Such calculations are expected to take the electron correlation of the 12 active electrons into account. Davidson's correction [23] for four-particle unlinked clusters is added to the CMRCI energies. The corresponding wavefunctions are expanded over 340 000–830 000 CSFs (C_{2v} symmetry) depending on the space and spin symmetries. All calculations were run on the Compaq alpha servers of the ULB/VUB computer center.

3. Electronic structure of NbCl from ab initio calculations

The potential energy curves of the 28 low-lying electronic states of NbCl have been obtained from CMRCI calculations performed at 8 internuclear distances equally distributed between 2.1 and 2.8 Å. Fig. 1 shows the potential curves of the lowest 9 quintet, 16 triplet, and 3 singlet states. The energy scale of this figure is relative to the minimum energy of the ground electronic state, which is predicted to have $^5\Pi$ symmetry. All the low-lying states of each spin and spatial symmetry have been characterized and this figure should thus provide a complete picture of the low-lying electronic structure of NbCl up to 15 000 cm^{-1}. The spectroscopic properties calculated for all these states are reported in Table 1: the equilibrium internuclear distances r_e, the harmonic frequencies at equilibrium ω_e, and the term energies T_0, corrected for the zero point energy contribution calculated within the harmonic approximation. Vertical term energies (values in parentheses in Table 1) were also calculated for a set of electronic states (4 triplet and 7 singlet states) above the limit of 15 000 cm^{-1}. These calculations were performed at an internuclear distance of 2.4 Å, close to the equilibrium distance of most electronic states of NbCl. We have also located the next states in the quintet system (2 $^5\Sigma^+$, 3 $^5\Delta$, 2 $^5\Phi$, 3 $^5\Sigma^-$, 1 $^5\Gamma$, and 4 $^5\Pi$), but they all lie above 35 000 cm^{-1} from the ground state. All these states arise from configurations with an open inner shell (2σ or 1π), which explains their high energies. States of septet spin symmetry also lie above 40 000 cm^{-1} for the same reason.

Table 2 provides an analysis of the CMRCI wavefunctions of all the calculated states in terms of a set of configurations, labeled from (A) to (S) and listed in Table 3. These configurations are those having a weight greater than or equal to 5% in the CMRCI wavefunctions, the weights being calculated as the sum of the squares of the CI coefficients of CSFs belonging to the corresponding electronic configurations. One sees that a high degree of configuration mixing occurs, particularly within the triplet spin system. This mixing prevents a clear separation between leading and secondary configurations. As will be discussed in more detail below, this situation makes the electronic structure of NbCl more intricate than that of VCl [4]. The strength of the configuration couplings also makes the convergence of the CASSCF/CMRCI calculations more difficult, which implied a systematic investigation of different alternative

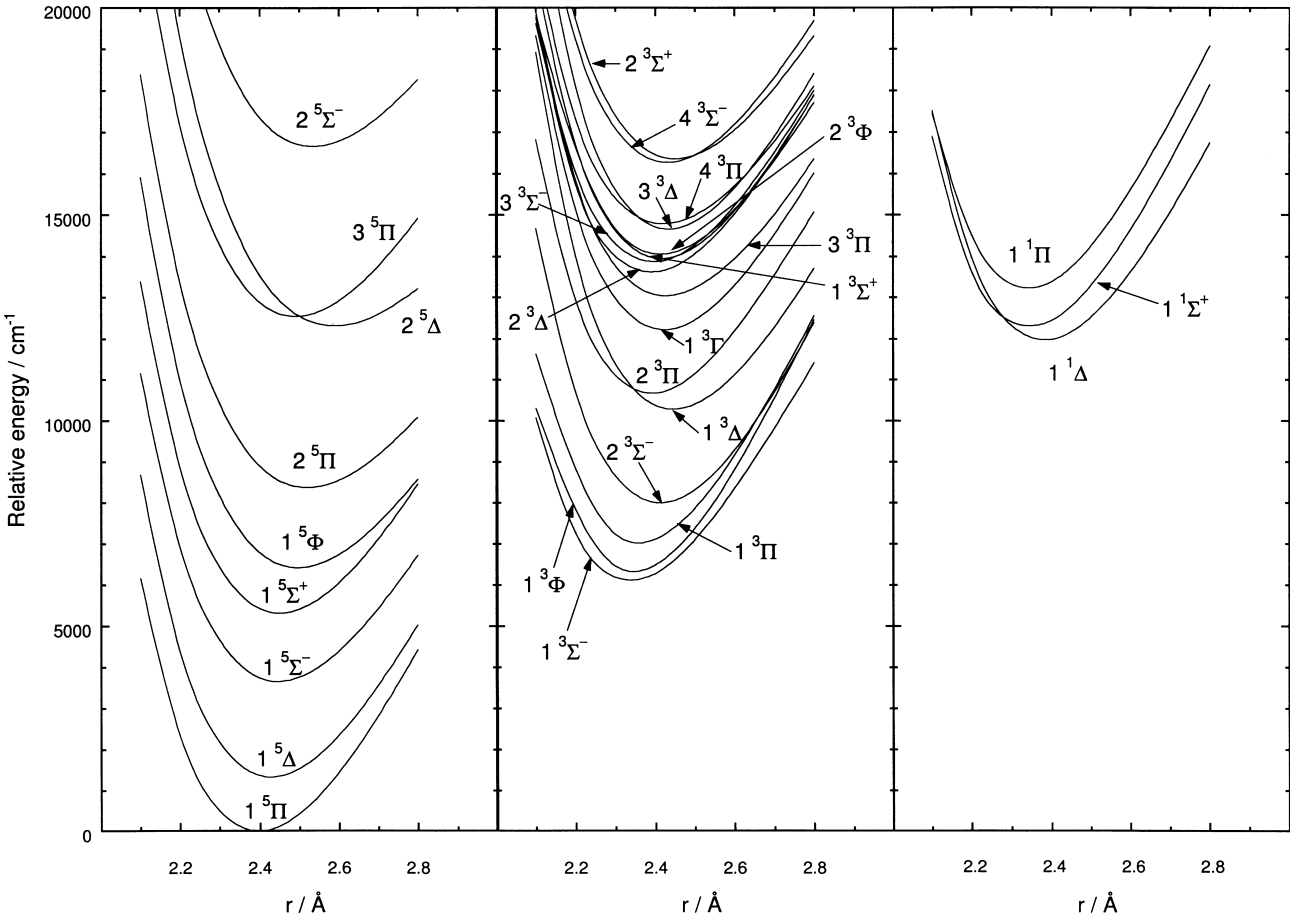

Fig. 1. The low-lying potential energy curves of NbCl in the quintet, triplet, and singlet spin systems from CMRCI calculations.

CASSCF orbital optimization schemes for each considered orbital and spin symmetry. We will not discuss in detail here these methodological tests which led to the final results reported in Tables 1 and 2, but simply say that the choice of states involved in the state averaging CASSCF optimization was found particularly important, and has been carefully investigated in order to balance properly all interacting states.

Let us now analyze the low-lying electronic structure of NbCl from our ab initio results, and compare it with the isovalent chloride, VCl [4]. Fig. 2 shows a correlation of calculated T_0 values between both chlorides. For the sake of clarity, we limit the comparison to the states below 10 000 cm^{-1} for the quintet and triplet systems, and to the two low-lying singlets. One sees first that the electrostatic splitting is in favor of the higher spin states in both systems. The quintet spin system is the lower, followed by the triplet system starting at about 6000 cm^{-1} in both chlorides, and the singlet system at about 17 000 and 12 000 cm^{-1}, respectively, in VCl and NbCl. The ground electronic state of NbCl is a $^5\Pi$ state arising from the configuration $3\sigma^1\ 1\delta^2\ 2\pi^1$, with a close lying ($\sim$1300 cm^{-1}) $^5\Delta$ state arising from the configuration $3\sigma^1\ 1\delta^1\ 2\pi^2$. The situation is inverted in VCl for which the energy difference is $\sim$500 cm^{-1}. Such differences are too small with respect to the limit of precision of our ab initio calculations to conclude firmly that the ground states of VCl and NbCl are different. Our findings are, however, consistent with the fact that the 1 $^5\Pi$–2 $^5\Pi$ energy difference is significantly smaller in NbCl (8300 cm^{-1}) than in VCl (10 400 cm^{-1}), while the opposite occurs for the 1 $^5\Delta$–2 $^5\Delta$ difference (12 300 and 8500 cm^{-1} for NbCl and VCl, respectively). The inter-state repulsions could thus explain the ground state inversion.

The next quintet states follow a similar pattern in both halides, but differences are observed in the spacing and ordering of the states. The first triplet state has the same $^3\Sigma^-$ symmetry in both systems and is located at about the same energy, but again the state spacing and ordering are not the same. As can be seen in Fig. 1, the density of triplet states is high between 12 000 and 17 000 cm^{-1} in NbCl. The analysis of the wavefunctions demonstrates the existence of fortuitous configuration quasi-degeneracies in NbCl. No similar degeneracies are observed in VCl [4] so its electronic structure is simpler. Let us take the two lowest $^5\Pi$ states as a single example. The configuration weights for NbCl (see Table 2) and VCl [4] are:

Table 1
Spectroscopic properties of the low-lying states of NbCl (from CMRCI calculations)

Multiplicity	State	T_0[a] (cm^{-1})	r_e (Å)	ω_e (cm^{-1})
5	$1\ ^5\Pi$	0	2.396	348
	$1\ ^5\Delta$	1326	2.427	337
	$1\ ^5\Sigma^-$	3643	2.446	318
	$1\ ^5\Sigma^+$	5311	2.450	324
	$1\ ^5\Phi$	6403	2.497	301
	$2\ ^5\Pi$	8346	2.520	287
	$2\ ^5\Delta$	12 273	2.590	266
	$3\ ^5\Pi$	12 528	2.492	311
	$2\ ^5\Sigma^-$	16 636	2.536	291
3	$1\ ^3\Sigma^-$	6119	2.350	349
	$1\ ^3\Phi$	6470	2.353	390
	$1\ ^3\Pi$	7039	2.366	388
	$2\ ^3\Sigma^-$	8004	2.412	347
	$1\ ^3\Delta$	10 281	2.445	337
	$2\ ^3\Pi$	10 672	2.391	353
	$1\ ^3\Gamma$	12 217	2.422	338
	$3\ ^3\Pi$	13 030	2.425	318
	$2\ ^3\Delta$	13 614	2.388	333
	$3\ ^3\Sigma^-$	13 866	2.395	336
	$1\ ^3\Sigma^+$	13 944	2.416	340
	$2\ ^3\Phi$	14 028	2.415	344
	$3\ ^3\Delta$	14 664	2.433	342
	$4\ ^3\Pi$	14 771	2.420	310
	$4\ ^3\Sigma^-$	16 265	2.431	325
	$2\ ^3\Sigma^+$	16 346	2.451	316
	$4\ ^3\Delta$	(16 009)	—	—
	$5\ ^3\Pi$	(16 030)	—	—
	$3\ ^3\Phi$	(17 402)	—	—
	$2\ ^3\Gamma$	(17 613)	—	—
1	$1\ ^1\Delta$	11 965	2.382	352
	$1\ ^1\Sigma^+$	12 301	2.350	363
	$1\ ^1\Pi$	13 231	2.350	366
	$2\ ^1\Delta$	(15 746)	—	—
	$1\ ^1\Gamma$	(16 084)	—	—
	$2\ ^1\Pi$	(16 338)	—	—
	$1\ ^1\Phi$	(16 542)	—	—
	$2\ ^1\Sigma^+$	(17 881)	—	—
	$2\ ^1\Gamma$	(19 540)	—	—
	$1\ ^1\Sigma^-$	(19 783)	—	—

[a] Values in parentheses are vertical term energies ($r = 2.4$ Å) of some selected electronic states of NbCl above 15 000 cm^{-1}.

Table 2
Analysis of the CMRCI wavefunctions of NbCl at $r = 2.4$ Å in terms of electronic configurations (see Table 3 for a definition of the configuration labeling)

Electronic state	Weight[a]
$1\ ^5\Pi$	60% (A) + 24% (I) + 10% (F)
$1\ ^5\Delta$	71% (B) + 23% (G)
$1\ ^5\Sigma^-$	89% (C) + 5% (H)
$1\ ^5\Sigma^+$	94% (D)
$1\ ^3\Sigma^-$	43% (J) + 30% (C) + 9% (B)
$1\ ^3\Phi$	73% (E) + 8% (F) + 8% (A)
$1\ ^5\Phi$	95% (F)
$1\ ^3\Pi$	51% (E) + 27% (A) + 6% (F)
$2\ ^3\Sigma^-$	38% (K) + 23% (B) + 16% (D) + 9% (C)+ 6% (J)
$2\ ^5\Pi$	49% (F) + 43% (I)
$1\ ^3\Delta$	89% (B)
$2\ ^3\Pi$	80% (A) + 5% (Q)
$1\ ^1\Delta$	27% (B) + 27% (K) + 15% (L) + 9% (D) + 5% (N)
$1\ ^3\Gamma$	64% (B) + 26% (C)
$1\ ^1\Sigma^+$	42% (J) + 22% (K) + 20% (B)
$2\ ^5\Delta$	71% (G) + 24% (B)
$3\ ^5\Pi$	36% (F)+ 32% (A) + 26% (I)
$3\ ^3\Pi$	51% (A) + 9% (O) + 8% (R) + 6% (E) + 5% (F) + 5% (I) + 5% (S)
$1\ ^1\Pi$	46% (E) + 21% (A) + 17% (F)
$2\ ^3\Delta$	61% (B) + 29% (M)
$3\ ^3\Sigma^-$	39% (C) + 34% (J) + 10% (K) + 7% (D)
$1\ ^3\Sigma^+$	81% (B) + 5% (D)
$2\ ^3\Phi$	50% (A) + 34% (F) + 6% (I)
$3\ ^3\Delta$	79% (B) + 6% (M) + 5% (D)
$4\ ^3\Pi$	50% (A) + 16% (F) +14% (R) + 7% (I)
$4\ ^3\Sigma^-$	40% (B) + 17% (C) + 15% (K) + 7% (D) + 7%(H)
$2\ ^3\Sigma^+$	75% (C) + 13% (H)
$2\ ^5\Sigma^-$	89% (H)+ 5% (C)
$2\ ^1\Delta$	44% (B) + 18% (L) + 14% (M) +8% (P) + 7% (N)
$4\ ^3\Delta$	36% (L) + 19% (B) + 18% (P) + 11% (N)
$5\ ^3\Pi$	52% (F) + 17% (A) + 7% (I) + 7% (E) + 6% (R)
$1\ ^1\Gamma$	74% (J) + 7% (C) + 6% (B)
$2\ ^1\Pi$	72% (A) + 5% (O)
$1\ ^1\Phi$	57% (A) + 22% (F) + 7% (E) + 6% (Q)
$3\ ^3\Phi$	69% (F) + 12% (A) + 5% (I)
$2\ ^3\Gamma$	71% (C) + 19% (B)
$2\ ^1\Sigma^+$	39% (B) + 14% (J) + 12% (D) + 12% (C) + 7% (G)
$2\ ^1\Gamma$	71% (B) + 9% (C) + 6% (G)
$1\ ^1\Sigma^-$	46% (B) + 46% (C)

[a] Weights (in percentage) are obtained from the square of the corresponding configuration interaction coefficients; weights lower than 5% are not reported.

$$\text{VCl}: \quad 1\ ^5\Pi = 62\%(\text{A}) + 32\%(\text{F}) \text{ and}$$
$$2\ ^5\Pi = 29\%(\text{A}) + 60\%(\text{F}) + 4\%(\text{I})$$

$$\text{NbCl}: \quad 1\ ^5\Pi = 60\%(\text{A}) + 10\%(\text{F}) + 24\%(\text{I}) \text{ and}$$
$$2\ ^5\Pi = 49\%(\text{F}) + 43\%(\text{I}).$$

The observed mixings suggest that a dominant (A)–(F) interaction occurs in VCl, with a weak interaction with the higher energy configuration (I), while in NbCl (I) and (F) are inverted and are nearly degenerate.

The valence MOs of NbCl, calculated at CASSCF level for the ground state, are drawn [24] in Fig. 3. One clearly sees that some MOs have a quasi-atomic character, while others have bonding or antibonding character. This is the case, for instance, for the 2σ and 4σ MOs, which are the corresponding bonding and antibonding mixing of the $3p\sigma$ orbital of Cl with the $5s\sigma$ and $4d\sigma$ orbitals of Nb. Another example is the antibonding combination of the chlorine $3p\pi$ orbital and niobium $4d\pi$ orbital in the 2π MO. The degree of ionicity can be calculated from a Mulliken population analysis of the CASSCF wavefunction. The degree of ionicity in the ground state, $\delta = 0.67$ electron charges, corresponds to an ionic $Nb^{+\delta}\ Cl^{-\delta}$ structure. This ionicity is comparable with the value of 0.65 calculated in the same way for VCl [4].

The final ab initio results which are useful for contributing to the assignment of the recorded spectra are

Table 3
Electronic configurations describing the calculated electronic states of NbCl (see Tables 1 and 2)

Labels	Configurations[a]
(A)	$3\sigma^1 1\delta^2 2\pi^1$
(B)	$3\sigma^1 1\delta^1 2\pi^2$
(C)	$3\sigma^1 1\delta^2 4\sigma^1$
(D)	$1\delta^2 2\pi^2$
(E)	$3\sigma^2 1\delta^1 2\pi^1$
(F)	$3\sigma^1 1\delta^1 2\pi^1 4\sigma^1$
(G)	$1\delta^1 2\pi^2 4\sigma^1$
(H)	$3\sigma^1 2\pi^2 4\sigma^1$
(I)	$1\delta^2 2\pi^1 4\sigma^1$
(J)	$3\sigma^2 1\delta^2$
(K)	$3\sigma^2 2\pi^2$
(L)	$3\sigma^2 1\delta^1 4\sigma^1$
(M)	$3\sigma^1 1\delta^3$
(N)	$1\delta^3 4\sigma^1$
(O)	$3\sigma^2 2\pi^1 4\sigma^1$
(P)	$3\sigma^1 1\delta^1 4\sigma^2$
(Q)	$1\delta^3 2\pi^1$
(R)	$3\sigma^1 2\pi^3$
(S)	$3\sigma^1 2\pi^1 4\sigma^2$

[a] All configurations have the same closed shell structure $1\sigma^2\ 2\sigma^2\ 1\pi^4$.

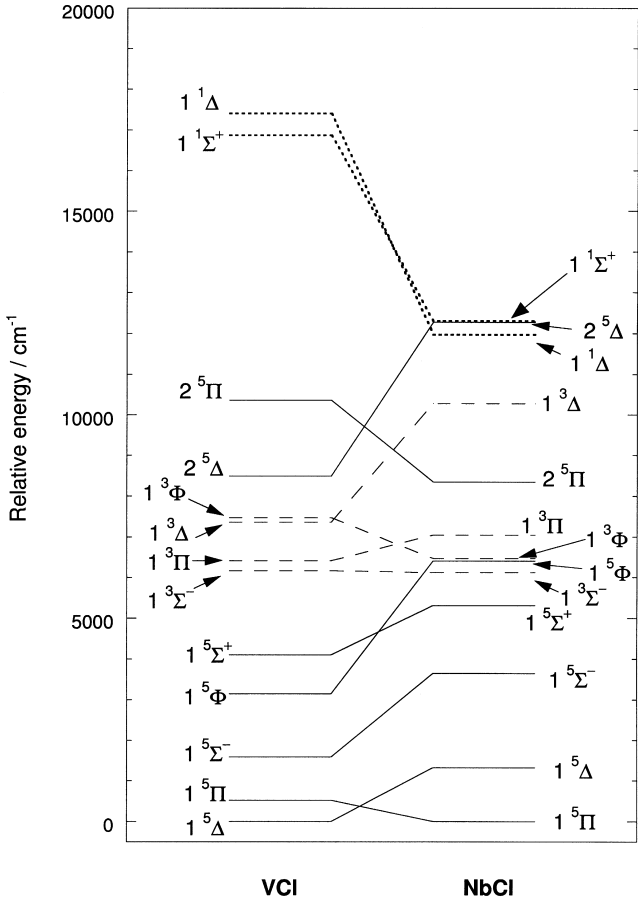

Fig. 2. Comparison of CMRCI term energy values T_0 between VCl [4] and NbCl.

the electric transition dipole moment values. Table 4 gives the electric dipole matrices calculated at the CMRCI level ($r = 2.4$ Å) for the low-lying quintet and triplet states. The diagonal elements of these matrices are the expectation values of the permanent electric dipole moments of the considered states. These quantities also reflect the ionic character of NbCl, with significant differences from state to state, in particular in the quintet system. The non-diagonal matrix elements (transition moments) will be used below in the discussion to characterize the most intense transitions.

4. Experimental

NbCl was excited in a microwave discharge lamp using a mixture of $NbCl_5$ vapor and about 3.5 Torr of He. The discharge tube was made of quartz and had an outside diameter of 12 mm. The emission from the lamp was sent directly into the entrance aperture of the 1-m Fourier transform spectrometer associated with the McMath-Pierce Solar Telescope of the National Solar Observatory.

For the 3000–10 000 cm^{-1} region the spectrometer was equipped with a CaF_2 beamsplitter, green glass filters, Si filters and InSb detectors. The spectra were recorded at 0.02 cm^{-1} resolution by co-adding 20 scans in 90 min of integration. The spectra in the 8000–14 000 cm^{-1} region were recorded using an RG715 filter and super blue Si detectors. This time 6 scans were co-added at 0.02 cm^{-1} resolution in about 80 min of integration. In the second experiment only three bands were initially observed near 1 μm. These bands were very weak in intensity and in order to observe additional bands, the spectrum in the 8800–12 200 cm^{-1} region was re-recorded using the UV beamsplitter, midrange Si diode detectors and RG850 red pass filter. This time 50 scans were coadded in about five hours of integration at a resolution of 0.02 cm^{-1}. This spectrum was much better than the previous one and several additional bands were observed with vibrational states in common. This new data has been very helpful in obtaining the correct rotational assignment of the different bands.

In addition to the NbCl bands, the observed spectra also contained Nb and He atomic lines as well as much stronger NbO and NbN molecular lines, although no O_2 or N_2 were added to the discharge cell. The 2–0 vibration–rotation band of HCl was also observed in the near infrared spectrum. The NbCl lines were easily distinguished from the lines belonging to NbO and NbN by the smaller line spacing in the branches.

The line positions were extracted from the observed spectra using a data reduction program called PC-DECOMP developed by J. Brault. The peak positions were determined by fitting a Voigt lineshape function to each spectral feature. The branches in the different sub-bands were sorted using a color Loomis–Wood program running on a PC computer. The measurements of the vibration–rotation lines of HCl [25] were used for the calibration of the bands near 6000 cm^{-1}. The spectrum

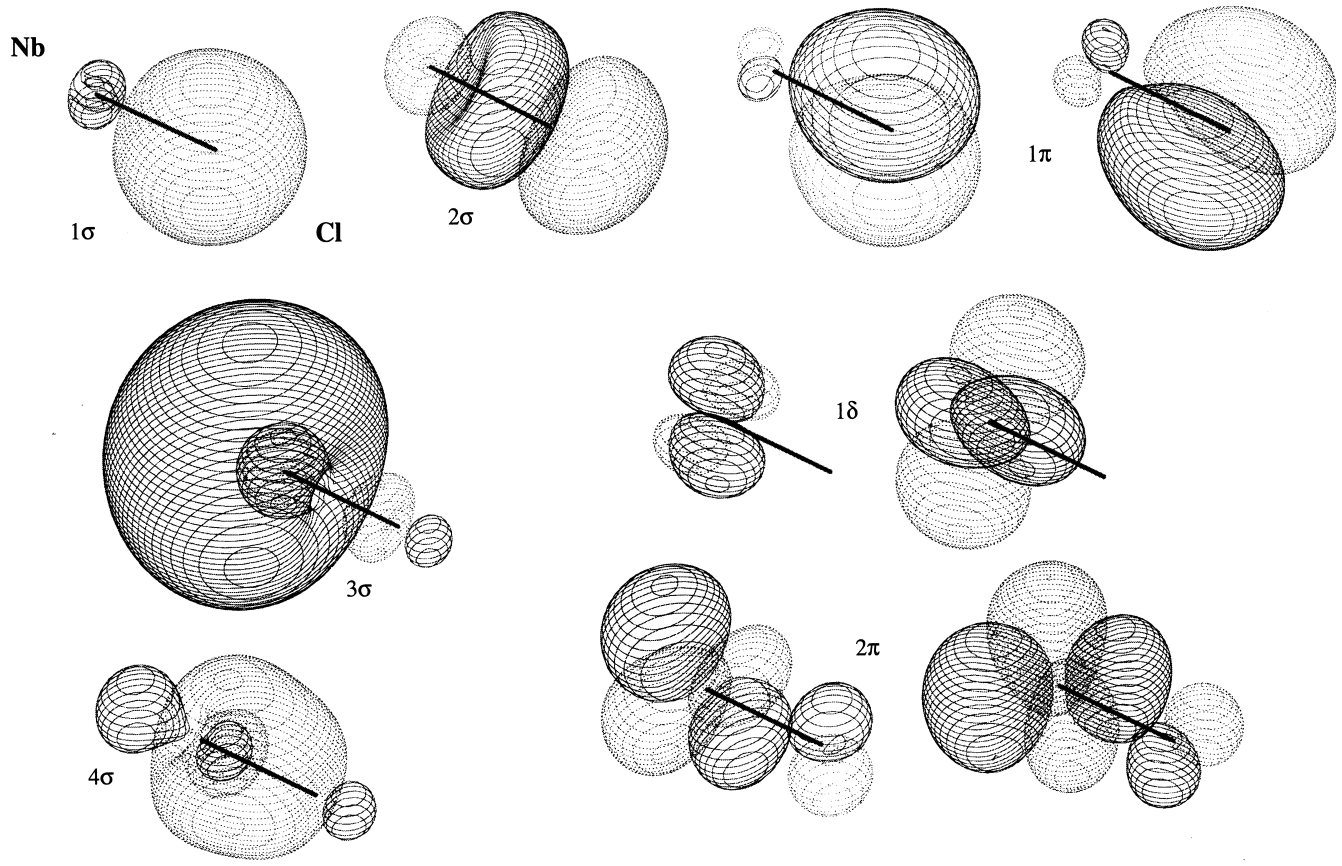

Fig. 3. Molecular orbitals calculated at CASSCF level for the ground $^5\Pi$ electronic state of NbCl at the equilibrium geometry (isocontour value of 0.02).

Table 4
Matrix elements of the electric dipole moment operator (in debye) within the quintet and triplet spin systems (from CMRCI calculations at $r = 2.4$ Å)

States	$1\,^5\Pi$	$2\,^5\Pi$	$3\,^5\Pi$	$1\,^5\Phi$	$1\,^5\Delta$	$2\,^5\Delta$	$1\,^5\Sigma^-$	$2\,^5\Sigma^-$	$1\,^5\Sigma^+$
$1\,^5\Pi$	5.37								
$2\,^5\Pi$	2.05	4.06							
$3\,^5\Pi$	0.99	0.36	2.74						
$1\,^5\Phi$	0	0	0	2.80					
$1\,^5\Delta$	0.02	0.53	0.45	0.65	5.50				
$2\,^5\Delta$	0.14	0.78	0.35	0.82	2.18	3.62			
$1\,^5\Sigma^-$	0.82	1.02	0.49	0	0	0	2.86		
$2\,^5\Sigma^-$	0.14	0.44	0.03	0	0	0	0.03	2.73	
$1\,^5\Sigma^+$	1.07	0.46	1.12	0	0	0	0	0	6.60
	$1\,^3\Pi$	$2\,^3\Pi$	$1\,^3\Phi$	$2\,^3\Phi$	$1\,^3\Delta$	$2\,^3\Delta$	$3\,^3\Delta$		
$1\,^3\Pi$	4.28								
$2\,^3\Pi$	0.46	4.62							
$1\,^3\Phi$	0	0	4.64						
$2\,^3\Phi$	0	0	0.16	3.06					
$1\,^3\Delta$	0.03	0.34	0.44	—	4.79				
$2\,^3\Delta$	0.13	0.45	0.16	—	0.26	4.33			
$3\,^3\Delta$	0.13	0.48	0.29	—	0.34	0.31	4.23		

in the 9800–11 000 cm^{-1} region was calibrated using common atomic and molecular lines observed in our previous experiments on NbN [7], which were calibrated using the Ne atomic line measurements of Palmer and Engelman [26]. The absolute accuracy of the wavenumber scale is expected to be of the order of $\pm 0.003\,cm^{-1}$. The NbCl lines in the stronger bands appear with a maximum signal-to-noise ratio of about six and have a typical linewidth of about $0.04\,cm^{-1}$. The precision of measurements of strong and unblended

NbCl lines is expected to be better than $\pm 0.003\,cm^{-1}$. The precision of measurements for the weaker and overlapped lines is limited to $\pm 0.005\,cm^{-1}$.

5. Observation and analysis

Apart from the NbO and NbN bands, our spectra consist of three groups of bands in the 4800–5800, 6500–7000, and 9800–11 000 cm^{-1} regions, which have been attributed to NbCl. The bands located in the 4800–5800 cm^{-1} could not be assigned due to their weak intensity. Several bands with pronounced R heads near 4954, 5145, 5230, 5303, 5460, 5586, 5707, and 5794 cm^{-1} remain unanalyzed. Most of these bands have P, Q, and R branches but their low J lines are affected by hyperfine effects making it difficult to obtain a rotational assignment. Much improved spectra are needed for the analysis of these bands. These bands probably belong to NbCl but the carrier of these bands cannot be established with certainty without a rotational analysis.

We have been able to obtain a rotational analysis of bands observed in the 6500–7000 and 9800–11 000 cm^{-1} regions. These two groups of bands have been assigned as the sub-bands of two different quintet–quintet transition without any state in common. The details of these transitions are provided in the following sections.

5.1. A $\Delta\Lambda = \pm 1$ transition in the 6500–7000 cm^{-1} region

Five bands observed in this region with R heads near 6533, 6704, 6799, 6862, and 6997 cm^{-1} have been assigned as 0–0 bands of the five sub-bands of a quintet–quintet transition. These bands consist of P, Q, and R branches with the Q branch being the most intense. This observation is consistent with a $\Delta\Lambda = \pm 1$ assignment for these sub-bands. The rotational lines in these bands do not have combination defects or Λ-doubling, suggesting that high Λ states ($\Lambda > 1$) must be involved. The rotational lines are unperturbed and show no hyperfine splittings in the range of observed J values. The electronic assignment of this transition remains uncertain as is the case with the Ω assignment of the different sub-bands. This transition probably involves a $^5\Phi$–$^5\Delta$ or $^5\Delta$–$^5\Phi$ transition although there are other possibilities. Two much weaker bands located near 6742 and 6945 cm^{-1} remain unanalyzed. These are probably the 1–1 bands of the 6799 and 6997 cm^{-1} sub-bands, respectively. Due to uncertainty in the electronic assignment of the bands of this transition, we will label the five sub-bands as sub-bands I–V in this paper.

5.2. A $\Delta\Lambda = 0$ transition in the 10 000–11 000 cm^{-1} region

A total of nine bands have been observed in the 9800–11 000 cm^{-1} region and have been classified into four sub-bands with 0–0 bands near 10 263, 10 409, 10 519, and 10 816 cm^{-1}. These bands consist of R and P branches consistent with a $\Delta\Lambda = 0$ transition. These bands are also free of Λ-doubling, consistent with high Λ ($\Lambda > 1$) assignment for the states. These bands are most probably the four sub-bands of a $^5\Delta$–$^5\Delta$ transition analogous to the $^5\Delta$–$^5\Delta$ near infrared transitions of VCl [3,4] and VF [5], but a $^5\Phi$–$^5\Phi$ assignment may not be completely ruled out. The Ω assignment in the different sub-bands was made on the basis of the relative magnitude of the rotational constants (B_v) in the states of different sub-bands, assuming regular states. The three bands with origins near 9874, 10 262, and 10 585 cm^{-1} have been assigned as the 0–1, 0–0, and 1–0 bands of the $^5\Delta_1$–$^5\Delta_1$ sub-band. It is somewhat surprising to note that no Λ-doubling was observed in these bands contrary to expectation for a $\Omega = 1$–1 transition with some Hund's case (c) character. This is possible if the lower and upper Ω states have negligible splitting or if the Λ splittings are similar in both states. This assignment provides the lower state vibrational interval of $\Delta G''_{1/2} = 388.2092(20)\,cm^{-1}$. Two bands with the origins near 10 130 and 10 518 cm^{-1} have been assigned as the 0–1 and 0–0 bands of the $^5\Delta_2$–$^5\Delta_2$ sub-band while other two bands with origins near 10 018 and 10 407 cm^{-1} have been assigned as the 0–1 and 0–0 bands of the $^5\Delta_3$–$^5\Delta_3$ sub-band. This assignment provides the $\Delta G''_{1/2}$ values of 388.1015(14) and 388.9976(27) cm^{-1} for the lower states with $\Omega = 2$ and 3, respectively. A band with the origin near 10 813 cm^{-1} has been assigned as the 0–0 band of the $^5\Delta_4$–$^5\Delta_4$ sub-band. The 0–1 band of this sub-band was not identified in our spectrum partly because of weak intensity and partly because of the presence of strong atomic lines near the predicted location. However, we have been able to identify the 0–2 band belonging to this sub-band which provides the $v'' = 2 - v'' = 0$ separation of 775.5190(15) cm^{-1} consistent with the $\Delta G''_{1/2}$ value observed from the other sub-bands. The bands belonging to the remaining sub-band, $^5\Delta_{0\pm}$–$^5\Delta_{0\pm}$, could not be identified in our spectra either due to their weak intensity or overlapping from neighboring bands. Because no Λ-doubling was resolved in any state, the Ω assignment is not secure. For example, the four spin-components that we observe could be $^5\Delta_3$, $^5\Delta_2$, $^5\Delta_1$, and $^5\Delta_0$ rather than $^5\Delta_4$, $^5\Delta_3$, $^5\Delta_2$, and $^5\Delta_1$, respectively. A part of the 10 518 cm^{-1} band is presented in Fig. 4 with the rotational lines of the main isotopomer $Nb^{35}Cl$ marked. An analysis of all the 1 μm bands indicates that none of the states are common with the states of the bands in the 6500–7000 cm^{-1} region. The rotational lines belonging to the minor isotopomer $Nb^{37}Cl$ were not measured due to their weak intensity.

The electronic states of NbCl are expected to have large spin–orbit splittings, so the molecular constants for the different Ω states have been determined separately by fitting the observed line positions to the customary empirical energy level expression:

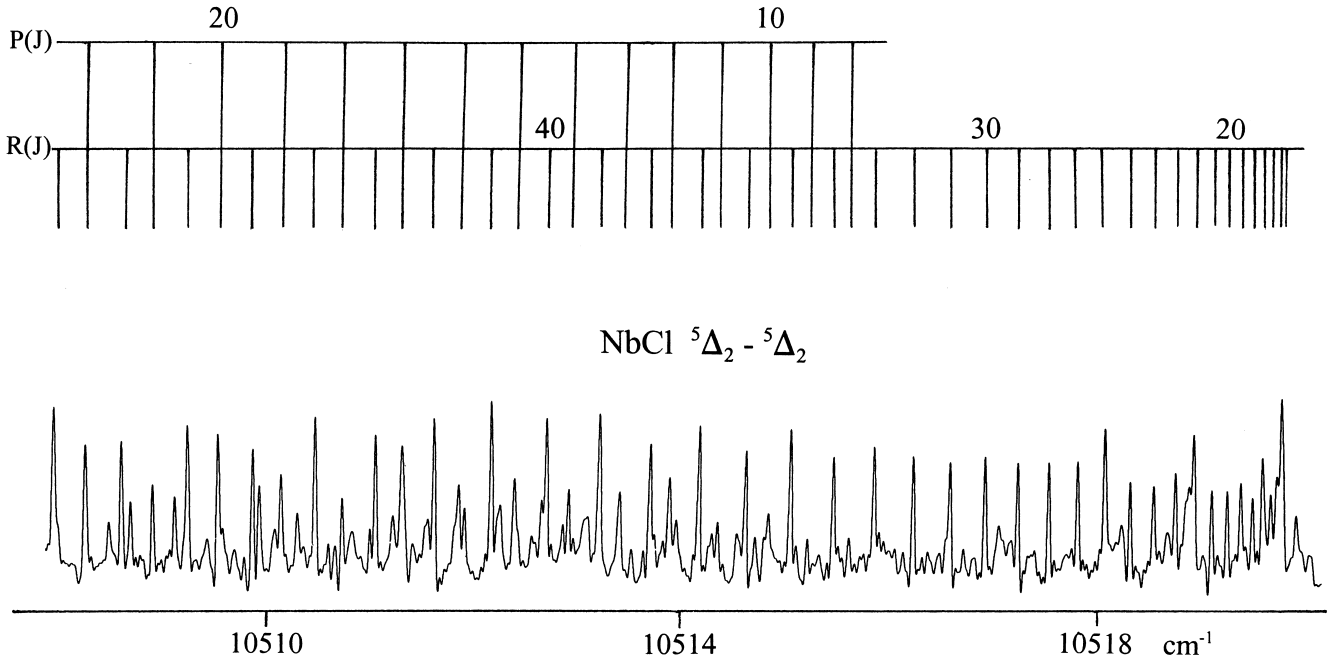

Fig. 4. A part of the 0–0 band of the $^5\Delta_2$–$^5\Delta_2$ sub-band of the transition near 1 μm.

$$F(J) = T_v + B_vJ(J+1) - D_v[J(J+1)]^2 + H_v[J(J+1)]^3.$$

In the final fit of lines of these bands, the blended and weaker lines were given lower weights depending on their signal-to-noise ratio and extent of blending. The observed line positions in these transitions can be obtained from the supplementary data available on-line [27] or from the authors upon request. The rotational constants obtained from the final fit of the observed lines in the two transitions are provided in Tables 5 and 6.

Table 5
Spectroscopic constants[a] (in cm^{-1}) for the $\Delta\Lambda = 1$ transition of NbCl (6500–7000 cm^{-1})

Sub-band[b]	T_{00}	B'_0	$10^8 \times D'_0$	B''_0	$10^8 \times D''_0$
I	6529.4734(13)	0.118198(29)	5.74(90)	0.121791(29)	4.68(96)
II	6700.72961(79)	0.1171479(63)	5.495(35)	0.1220165(62)	5.170(35)
III	6795.2748(14)	0.117825(11)	6.114(68)	0.122165(11)	5.130(67)
IV	6857.8591(24)	0.118711(22)	7.07(19)	0.122427(22)	5.72(19)
V	6991.3712(12)	0.116359(13)	5.92(12)	0.121542(13)	5.38(12)

[a] The values in parentheses are one standard deviation in the last two digits.
[b] The electronic and Ω assignments are uncertain.

Table 6
Rotational constants[a](in cm^{-1}) for the $^5\Delta$–$^5\Delta$ system of NbCl (9000–11 000 cm^{-1})

Constants	$\Omega' = 1$		$\Omega' = 2$		$\Omega' = 3$		$\Omega' = 4$		
	$v = 0$	$v = 1$	$v = 0$	$v = 1$	$v = 0$	$v = 1$	$v = 0$	$v = 1$	$v = 2$
T_{vv}	10262.3502(21)	10585.1405(12)	10518.07071(75)	—	10407.1195(18)	—	10813.3779(11)	—	—
B_v	0.1151601(80)	0.1147340(82)	0.1171059(53)	—	0.117708(17)	—	0.1213700(78)	—	—
$10^7 \times D_v$	0.857(30)	0.167(34)	0.6430(67)	—	−1.148(71)	—	0.353(12)	—	—
$10^7 \times H_v$	1.652(53)	0.305(68)	−0.1842(36)	—	—	—	—	—	—
	$\Omega'' = 1$		$\Omega'' = 2$		$\Omega'' = 3$		$\Omega'' = 4$		
T_{vv}	0	388.2092(20)	0	388.0989(10)	0	388.9964(27)	0	—	775.5160(14)
B_v	0.1259133(75)	0.1253840(76)	0.1262248(53)	0.1256716(53)	0.126346(18)	0.125812(18)	0.1263235(79)	—	0.1252257(79)
$10^7 \times D_v$	0.481(19)	0.514(19)	0.5581(61)	0.5490(60)	0.602(76)	0.743(79)	0.509(12)	—	0.523(12)

[a] The values in parentheses are one standard deviation in the last two digits.

6. Discussion

Prior to the present work there was no experimental work or detailed theoretical study of NbCl reported in the literature, although some limited theoretical predictions are available for the related NbH [28] and TaH [29] molecules, as well as Siegbahn's survey of 4*d* metal hydrides and halides [8]. The spectroscopic properties of a number of low-lying electronic states of NbH were calculated by Das and Balasubramanian [28], who predicted a $^5\Delta$ ground state for NbH. A similar study of TaH by Cheng and Balasubramanian [29] predicted a $\Omega = 0^+$ ground state which is a mixture of $^5\Delta(0^+)$, $^5\Pi(0^+)$, $^3\Pi(0^+)$, and $^3\Sigma^-(0^+)$ states. As has been described earlier, we have observed two transitions ($\Delta\Lambda = \pm 1$ and 0) in the 6500–7000 and 9800–11 000 cm^{-1} regions, respectively, which do not have any state in common. The calculations on NbH [28] and TaH [29] were not of much help in the assignment of the near infrared transitions of NbCl, although our previous work on isovalent VCl [4] suggests a $^5\Delta$–$^5\Delta$ assignment for the NbCl transition observed near 1 μm.

We have performed our own ab initio calculations on NbCl to assist us in the assignments, but have found that our experimental observations are not fully explained by the ab initio results. Our calculations predict a $^5\Pi$ ground state for NbCl with a close-lying $^5\Delta$ state located at 1326 cm^{-1} above the ground state, although a $^5\Delta$ ground state cannot be ruled out. The ab initio predictions for the transition dipole moments (Table 4) provide useful information for the electronic assignment of the observed transitions. The non-diagonal elements in this Table are the transition dipole moment values, and the squared values are related to electronic transition intensities. The most intense transitions are found within the quintet spin system and correspond to the $2\ ^5\Delta \rightarrow 1\ ^5\Delta$ and $2\ ^5\Pi \rightarrow 1\ ^5\Pi$ transitions. We have assigned the 1 μm transition as the $2\ ^5\Delta \rightarrow 1\ ^5\Delta$ transition. Contrary to the prediction, we do not see any sign of the $2\ ^5\Pi \rightarrow 1\ ^5\Pi$ transition, which involves the predicted ground state, and is expected to be nearly as strong as the $2\ ^5\Delta \rightarrow 1\ ^5\Delta$ transition. Instead, we find a $\Delta\Lambda = \pm 1 (\Lambda > 1)$ transition in the 6500–7000 cm^{-1} region that cannot be explained on the basis of our theoretical results.

The main difficulty is that all suitable low-lying transitions such as $1\ ^5\Phi$–$1\ ^5\Delta$, have a state in common with the $2\ ^5\Delta$–$1\ ^5\Delta$ transition. These assignments are definitely ruled out because the two analyzed transitions do not have any states in common. Perhaps the $\Delta\Lambda = \pm 1$ transition is between two higher-lying states. Another possibility is that strong spin–orbit effects have somehow altered the energy level and/or the intensity pattern. Based on our previous experience, this latter possibility does not seem very likely, but we intend to carry out some new ab initio calculations that include spin–orbit coupling.

The constants of Tables 5 and 6 have been used to determine approximate Hund's case (a) values by taking simple averages of the values of the different spin components of the observed states. The B_0 values for the upper and lower states of the 6500–7000 cm^{-1} transition are $B'_0 = 0.11765\ cm^{-1}$, $B''_0 = 0.12199\ cm^{-1}$, respectively. The observation of $v = 1$ vibrational levels in a number of sub-bands of the $^5\Delta$–$^5\Delta$ transition (Table 6) have enabled us to determine the approximate values of $B''_0 = 0.12620$ and $B''_1 = 0.12566\ cm^{-1}$ for the lower $^5\Delta$ state. These constants provide equilibrium constants of $B''_e = 0.12647\ cm^{-1}$, $\alpha''_e = 0.00054\ cm^{-1}$ and $r''_e = 2.2905$ Å for the $1\ ^5\Delta$ state. These observations also provide the vibrational interval of 388.44 cm^{-1} for the lower $^5\Delta$ state. In contrast to our previous work, the experimental values for the observed $^5\Delta$ states are in only modest agreement with the values predicted by our ab initio calculations. For example, the values of $r''_e = 2.2905$ Å and $\Delta G_{1/2} = 388.44\ cm^{-1}$ have been obtained from the experiment whereas the ab initio values of the equilibrium bond length and the vibrational constant are $r''_e = 2.427$ Å and $\omega_e = 337\ cm^{-1}$. Our planned ab initio calculations that will explicitly include spin–orbit effects may provide better agreement between experiment and theory.

7. Conclusions

We have recorded the emission spectrum of NbCl in the 3000–20 000 cm^{-1} region using a Fourier transform spectrometer. Two groups of bands observed in the 6500–7000 and 9800–11 000 cm^{-1} regions have been attributed to NbCl and have been assigned as due to two electronic transitions having no state in common. Five bands observed in the 6500–7000 cm^{-1} interval have been assigned as the sub-bands of a $\Delta\Lambda = \pm 1$ transition with $\Lambda > 1$. The bands observed in the 9800–11 000 cm^{-1} region have been assigned as the four sub-bands of a $\Delta\Lambda = 0$ transition, which has been assigned as a $^5\Delta$–$^5\Delta$ transition. The spectroscopic properties of the low-lying electronic states of NbCl have also been predicted and compared with experimental results. It has been noted that the theoretical results do not fully support the experimental observations and further ab initio calculations that will include spin–orbit effects are planned.

Acknowledgments

We thank M. Dulick and D. Branston of the National Solar Observatory for assistance in obtaining the spectra. The National Solar Observatory is operated by the Association of Universities for Research in Astronomy, under contract with the National Science Foundation.

The research described here was supported by funding from the NASA laboratory astrophysics program. Support was also provided by the Natural Sciences and Engineering Research Council of Canada and by the Fonds National de le Recherche Scientifique de Belgique. N. R. thanks the F.R.I.A. (Belgium) for a Ph.D. Grant.

References

[1] K. Eller, H. Schwarz, Chem. Rev. 91 (1991) 1121.
[2] C.W. Bauschlicher Jr., S.P. Walch, S.R. Langhoff, in: A. Veillard (Ed.), Quantum Chemistry: The Challenge of Transition Metals and Coordination Chemistry, NATO ASI Ser. C, Reidel, Dordrecht, 1986.
[3] R.S. Ram, P.F. Bernath, S.P. Davis, J. Chem. Phys. 114 (2001) 4457–4460.
[4] R.S. Ram, J. Liévin, P.F. Bernath, S.P. Davis, J. Mol. Spectrosc. 217 (2003) 186–194.
[5] R.S. Ram, P.F. Bernath, S.P. Davis, J. Chem. Phys. 116 (2002) 7035–7039.
[6] O. Launila, B. Schimmelpfennig, H. Fagerli, O. Gropen, A.G. Taklif, U. Wahlgren, J. Mol. Spectrosc. 186 (1997) 131–143, and references therein.
[7] R.S. Ram, P.F. Bernath, J. Mol. Spectrosc. 201 (2000) 267–279, and references therein.
[8] P.E.M. Siegbahn, Theor. Chim. Acta 86 (1993) 219.
[9] N.P. Galkin et al., Zh. Fiz. Khim. 45 (1971) 2695.
[10] R.S. Ram, J. Liévin, P.F. Bernath, J. Chem. Phys. 109 (1998) 6329–6337.
[11] R.S. Ram, J. Liévin, P.F. Bernath, J. Chem. Phys. 111 (1999) 3449–3456.
[12] R.S. Ram, J. Liévin, P.F. Bernath, J. Mol. Spectrosc. 197 (1999) 133–146.
[13] R.S. Ram, J. Liévin, P.F. Bernath, J. Mol. Spectrosc. 215 (2002) 275–284.
[14] R.S. Ram, J. Liévin, G. Li, T. Hirao, P.F. Bernath, Chem. Phys. Lett. 343 (2001) 437–445.
[15] R.S. Ram, A.G. Adam, A. Tsouli, J. Liévin, P.F. Bernath, J. Mol. Spectrosc. 202 (2000) 116–130.
[16] R.S. Ram, A.G. Adam, W. Sha, A. Tsouli, J. Liévin, P.F. Bernath, J. Chem. Phys. 114 (2001) 3977–3987.
[17] H.-J. Werner, P.J. Knowles, J. Chem. Phys. 82 (1985) 5053–5063; P.J. Knowles, H.-J. Werner, Chem. Phys. Lett. 115 (1985) 259–267.
[18] H.-J. Werner, P.J. Knowles, J. Chem. Phys. 89 (1988) 5803–5814; P.J. Knowles, H.-J. Werner, Chem. Phys. Lett. 145 (1988) 514–522.
[19] MOLPRO (version 2000.1) is a package of ab initio programs written by H.-J. Werner, P.J. Knowles, with contributions from R.D. Amos, A. Bernhardsson, A. Berning, P. Celani, D.L. Cooper, M.J.O. Deegan, A.J. Dobbyn, F. Eckert, C. Hampel, G. Hetzer, T. Korona, R. Lindh, A.W. Lloyd, S.J. McNicholas, F.R. Manby, W. Meyer, M.E. Mura, A. Nicklass, P. Palmieri, R. Pitzer, G. Rauhut, M. Schütz, H. Stoll, A.J. Stone, R. Tarroni, T. Thorsteinsson.
[20] D. Andrae, U. Häussermann, M. Dolg, H. Stoll, H. Preuss, Theor. Chim. Acta 77 (1990) 123–141.
[21] A. Bergner, M. Dolg, W. Kuechle, H. Stoll, H. Preuss, Mol. Phys. 80 (1993) 1431–1441.
[22] D.E. Woon, T.H. Dunning Jr., J. Chem. Phys. 98 (1993) 1358–1371.
[23] S.R. Langhoff, E.R. Davidson, Int. J. Quantum Chem. 8 (1974) 61–74.
[24] G. Schaftenaar, J.H. Noordik, J. Comput. Aided Mol. Design 14 (2000) 123.
[25] R.B. LeBlanc, J.B. White, P.F. Bernath, J. Mol. Spectrosc. 164 (1994) 185–191.
[26] B.A. Palmer, R. Engleman, Atlas of the Thorium Spectrum, Los Alamos National Laboratory, Los Alamos, 1983.
[27] Supplementary data can be found in the JMS electronic archive. Available from http://www.apnet.com/www/journal/ms.htm or http://msa.lib.ohio-state.edu/jmsa_hp.htm.
[28] K.K. Das, K. Balasubramanian, J. Mol. Spectrosc. 144 (1990) 245–256.
[29] W. Cheng, K. Balasubramanian, J. Mol. Spectrosc. 149 (1991) 99–108.